Local evidence for collective spin excitations in the distorted kagome antiferromagnet Pr_3BWO_9

K. Y. Zeng,[1,2] F. Y. Song,[3] Z. M. Tian,[3,*] Qiao Chen,[4] Shun Wang,[4] Bo Liu,[5,6] Shiliang Li,[5,6] L. S. Ling,[1] W. Tong,[1] Long Ma,[1,†] and Li Pi[1,2]

[1]*Anhui Province Key Laboratory of Condensed Matter Physics at Extreme Conditions, High Magnetic Field Laboratory, Chinese Academy of Sciences, Hefei 230031, China*

[2]*Hefei National Laboratory for Physical Sciences at the Microscale, University of Science and Technology of China, Hefei 230026, China*

[3]*School of Physics and Wuhan National High Magnetic Field Center, Huazhong University of Science and Technology, Wuhan 430074, China*

[4]*School of Physics and MOE Key Laboratory of Fundamental Physical quantum Physics, PGMF, Huazhong University of Science and Technology, Wuhan 430074, China*

[5]*Beijing National Laboratory for Condensed Matter Physics, Institute of Physics, Chinese Academy of Sciences, Beijing 100190, China*

[6]*School of Physical Sciences, University of Chinese Academy of Sciences, Beijing 100190, China*

(Received 21 July 2021; revised 14 September 2021; accepted 18 October 2021; published 27 October 2021)

We report a local probe investigation of the frustrated antiferromagnet Pr_3BWO_9 with a distorted kagome lattice. The absence of magnetic order or spin-freezing is indicated by a spectral analysis down to 0.3 K and by specific heat measurements down to 0.09 K. The Knight shifts show an upturn behavior with the sample cooling down, which is further suppressed by the external field. For the spin dynamics, gapped spin excitation is observed from the temperature dependence of spin-lattice relaxation rates, with the gap size proportional to the applied magnetic field intensity. Comparatively, an unexpected sharp peak is observed in the nuclear spin-spin relaxation rate data at $T^* \sim 4$–5 K. These results indicate an unconventional persistent fluctuating paramagnetic ground state with antiferromagnetic collective spin excitations in the strongly frustrated spin system.

DOI: 10.1103/PhysRevB.104.155150

I. INTRODUCTION

Geometrical frustration has triggered enormous research interest in recent years, not only for the possible relationship with high-T_c superconductivity but also for the interesting ground states and exotic quantum excitations in their own right [1]. For antiferromagnetically coupled spins located at triangles, the antiparallel configuration favored by the nearest interaction cannot be simultaneously fulfilled, leading to very large degeneracy of ground states as well as strong quantum fluctuations. One of the most intriguing ground states is the quantum spin liquid (QSL) [1], where the spins dynamically entangle with each other but never order even at zero temperature. Among various types of QSLs proposed by theory, the common feature for telling QSLs from other states is deconfined spinon excitations with fractional quantum numbers. As a result, research into the low-energy spin excitation property is of great importance in the study of frustrated antiferromagnets.

Compared with the edge-shared triangular lattice, corner-shared triangles (kagome lattices) with low coordination and weak second-neighbor interaction possess a stronger magnetic frustration effect and, thus, are more attractive. In the last decade, $ZnCu_3(OH)_6Cl_2$ is the intensively studied promising kagome lattice realizing the QSL state [2], where continuous spin excitation [3] and fingerprints of fractional spinons [1] have been observed. However, two inherent drawbacks exist in $ZnCu_3(OH)_6Cl_2$. One is the natural mixing of Cu^{2+} and Zn^{2+} due to their similar ion radii [4], complicating investigation of the intrinsic properties of the QSL state. The other is the near-impossibility of chemical substitution at the magnetic sites, prohibiting further exploration of other novel states and excitations in this system.

For magnetic lanthanide ions, the local crystal electric field (CEF) splits the spin-orbit entangled J momentum space into $2J + 1$ states and, finally, determines the single-ion anisotropy with an effective J_{eff}. By locating different lanthanide ions on the kagome lattice, various novel ground states and spin excitations can be realized, relying on different spin anisotropy, spin-orbit coupling and exchange, and dipolar interaction. The rare-earth-based $Ln_3M_2Sb_3O_{14}$ (Ln = lanthanide, M = Mg or Zn) with a kagome lattice is a precise example for testing this judgment [5]. For $Dy_3Mg_2Sb_3O_{14}$ with anisotropic Ising spins, the kagome spin ice with a "two-in-one-out" or "one-in-two-out" magnetic structure is identified by neutron scattering [6], while for the Ln = Ho case, a new quantum state with both characteristics of classical spin ice and quantum fluctuation and tunneling is found [7]. For the Ln = Gd case with isotropic large Heisenberg large spins, a dipolar interaction may result in the observed magnetic ordered state with a 120° structure [5,8]. Recently, a possible QSL state is proposed based on the persistent strong low-energy spin excitations down to $T = 50$ mK by muon spin rotation (μSR) and the magnetic contribution to the linear temperature dependence

*tianzhaoming@hust.edu.cn
†malong@hmfl.ac.cn

of the heat capacity [9]. Controversially, the random mixing of Tm^{3+} and Zn^{2+} was observed very recently [10], which may lead to the mimicry of QSLs. Thus, the rare-earth-based kagome lattice has supplied a new playground for exploring exotic frustrated quantum states.

To overcome the possible antisite disorder, some of us have synthesized a new family of rare-earth-based antiferromagnets, Ln_3BWO_9 (Ln = Pr, Nd, Gd-Ho), with the lanthanide ions located on the distorted kagome structure in the *ab* plane and stacking in an *AB*-type fashion along the *c* axis [11]. A dc magnetization analysis suggests similar magnetic behaviors with other rare-earth-based frustrated antiferromagnets [11]. However, no further study on the ground state and spin excitations has been reported up to now.

In this article, we employ nuclear magnetic resonance (NMR) as a local probe to study the spin excitations in the lanthanide frustrated antiferromagnet Pr_3BWO_9 with a distorted kagome lattice. The paramagnetic state persists without any magnetic ordering or spin-freezing as evidenced by ^{11}B spectral analysis down to $T = 0.3$ K and by specific heat measurements down to $T = 0.09$ K, far below its Curie-Weiss temperature. The Knight shifts measuring spin correlations at $\mathbf{q} = 0$ show an upturn behavior with the sample cooling down, which is further suppressed by the external field. For the spin dynamics, thermally activated behavior is observed in the temperature dependence of spin-lattice relaxation rates, indicating gapped spin excitations. The gap size is proportional to the field intensity in both field directions, but with very different slopes, demonstrating the spin anisotropy. Comparatively, an unexpected sharp peak is observed in the nuclear spin-spin relaxation rate data at $T^* \sim 4$–5 K, which is contributed by the hyperfine field fluctuation parallel to the applied magnetic direction. These results indicate a cooperative paramagnetic state with short-ranged collective excitations in the strongly frustrated spin system.

II. MATERIALS AND METHODS

Single crystals of Pr_3BWO_9 were synthesized by the conventional flux method. For NMR studies, crystals with typical dimensions of $1.5 \times 1.5 \times 0.2$ mm^3 are used. Our NMR measurements are conducted on ^{11}B nuclei ($\gamma_n = 13.655$ MHz/T, $I = 3/2$) with a phase-coherent NMR spectrometer. The spectra are obtained by summing up or integrating the spectral weight by sweeping the frequency under fixed magnetic fields. The measurement of spin-lattice relaxation rates is performed by the inversion-recovery method. The spin-spin relaxation rates are obtained by measuring the nuclear transverse dephasing with the two-pulse Hahn echo sequence.

The crystal structure of Pr_3BWO_9 is built up by blocks of PrO_8, WO_6, and BO_3 polyhedra in the corner- or edge-sharing manner [11]. There is only one Wyckoff position for Pr, W, and B sites. The BO_3 trigons share edges with the PrO_8 polyhedra, leading to a very strong hyperfine coupling between ^{11}B nuclei and magnetic moments. A top view of the crystal structure along the *c* axis is shown in Fig. 1(a). The magnetic Pr^{3+} sites form a distorted kagome structure in the crystalline *ab* plane, which is intentionally shown by bold red lines.

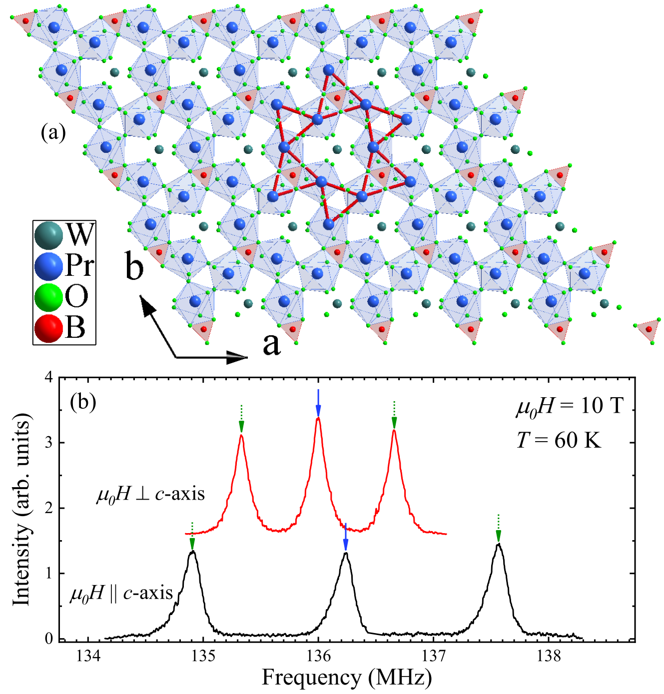

FIG. 1. (a) The crystalline structure of Pr_3BWO_9 as seen against the *c* axis. The distorted kagome lattice is shown by the bold red lines. (b) Typical ^{11}B NMR spectra with the magnetic field applied perpendicular or parallel to the *c* axis of the single crystal. The central and satellite transitions are shown by the solid blue and dotted green arrows, respectively.

III. RESULTS

A. NMR Spectral Analysis

In Fig. 1(b), we show typical ^{11}B NMR spectra at $T = 60$ K with a 10-T field along different directions. Both spectra are composed of three peaks, one at the frequency center and the other two located symmetrically at both sides. For nuclei with spin $I = 3/2$ in a nonzero local electric field gradient (EFG) under strong magnetic fields, the first-order correction to the Zeeman energy term due to quadruple interactions splits the single NMR transition into three, respectively, named the central transition and satellites [12,13]. The frequency of satellites strongly depends on the angle θ between the applied field and the pricipal axis of the EFG tensor. For the present sample without *ab*-plane EFG anisotropy (confirmed by in-plane angle rotational data not shown), the correction to the frequency can be written as $\nu_m^{(1)} = \nu_Q(m - 1/2)(3\cos^2\theta - 1)/2$, where ν_Q and m denote the quadruple frequency and nuclear magnetic quantum number, respectively. The ν_Q value is calculated to be $\sim$1.325 MHz at $T = 60$ K, and the main axis of the EFG is along the crystalline *c* axis. These observations are fully consistent with the crystal structure symmetry.

The full NMR spectra at different temperatures with the magnetic field applied parallel or perpendicular to the *c* axis are shown in Figs. 2(a) and 2(b). In both field directions, all three peaks shift to the lower-frequency side and broaden gradually with the sample cooling down. For $T = 0.3$ K, far below the Curie-Weiss temperature ($|\theta_{\rm cw}| = 6.1$ K for $\mu_0 H \perp c$ and $|\theta_{\rm cw}| = 5.4$ K for $\mu_0 H || c$, as shown by the

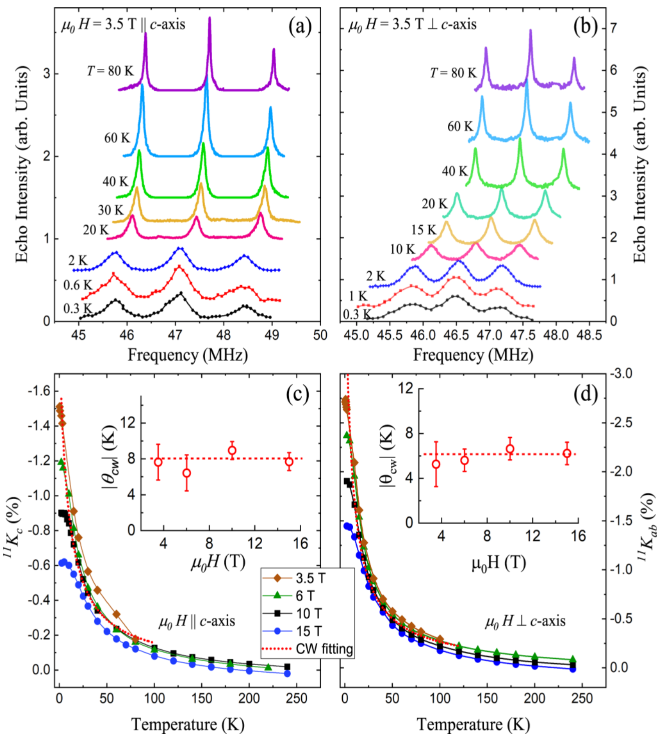

FIG. 2. The frequency-swept ^{11}B NMR spectra at different temperatures with a 3.5-T field applied along (a) or perpendicular to (b) the c axis. (c, d) The temperature dependence of the ^{11}B Knight shift ^{11}K under different magnetic fields. Dotted lines are fits to the Curie-Weiss function. Inset: Plots of the absolute values of the obtained Curie-Weiss temperatures ($|\theta_{cw}|$) as a function of the field intensity.

single-crystal dc susceptibility [14]), the main feature of the spectrum is maintained as that at much higher temperatures. No further line splitting or amplitude modulation is observed in the present sample. We note that the hyperfine coupling between ^{11}B nuclei and the magnetic sites is very strong as evidenced by the enormous Knight shift and ultrafast spin-lattice relaxation (shown later). Any magnetic ordering of the commensurate or incommensurate type or spin-freezing, if present, is very unlikely to be missed in the low-temperature spectra for both field directions. Additionally, no magnetic transition is observed from the specific heat measurements down to 0.09 K [14]. Thus, our data support a paramagnetic state in Pr_3BWO_9 with the temperature down to at least $0.017|\theta_{cw}|$, demonstrating strong magnetic frustration.

The intrinsic local spin susceptibility can be measured by the Knight shift, suffering less from the impurity effect than bulk probes. The temperature dependence of the Knight shift for different magnetic fields is shown in Figs. 2(c) and 2(d). The Knight shifts (^{11}K) are calculated as the relative line shift of the central transition with respect to the Larmor frequency, after removing the second-order correction arising from quadruple interaction. With the sample cooling down, all the Knight shifts share a similar Curie-Weiss upturn behavior with dc susceptibility. Fittings with the equation $^{11}K \propto 1/(T-\theta_{cw})$ to the low-temperature data yield a nearly field-independent $|\theta_{cw}|$ value (shown in the insets). The θ_{cw} is calculated to be ~ -6 K for $\mu_0 H \perp c$ and ~ -8 K for $\mu_0 H || c$, again demonstrating a moderate antiferromagnetic coupling strength. With increasing field intensity, the Knight shift tends to level off at low temperatures. This results from the saturated paramagnetic Pr^{3+} magnetic moments, which are also observed in other frustrated [15–17] or Kitaev antiferromagnets [18].

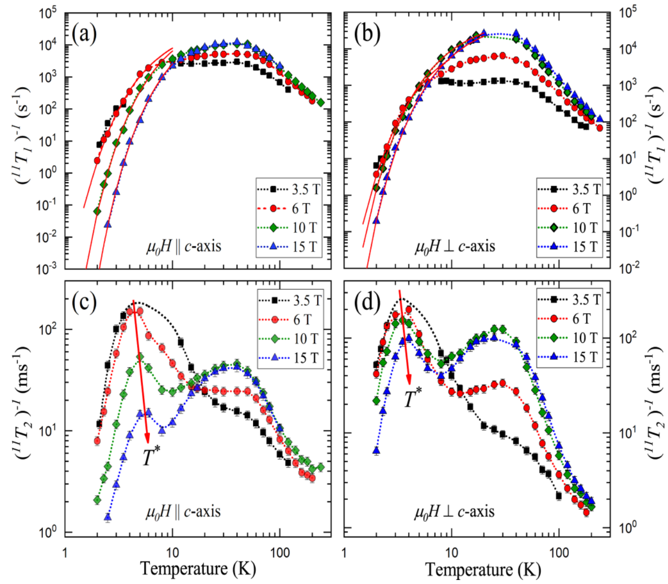

FIG. 3. (a, b) Spin-lattice relaxation rates ($1/^{11}T_1$) as a function of the temperature under different magnetic fields with $\mu_0 H || c$ or $\mu_0 H \perp c$. Solid red lines are representative fits to $1/T_1 \propto \exp(-\Delta/T)$ (see the text). (c, d) Spin-spin relaxation rates ($1/^{11}T_2$) as a function of the temperature under different magnetic fields with $\mu_0 H || c$ or $\mu_0 H \perp c$.

B. The Spin Dynamics

To further explore the spin dynamics in Pr_3BWO_9, we have measured both nuclear spin-lattice and spin-spin relaxation rates ($1/^{11}T_1$ and $1/^{11}T_2$) and show their temperature dependence under different magnetic fields in Fig. 3. Both measurements are made at the central peak. The $1/^{11}T_1$ is obtained by fitting the nuclear magnetization to the function, $M(t)/M(\infty) = 1 - 0.1\exp(-t/T_1) - 0.9\exp(-6t/T_1)$, the standard recovery function for the central transition of nuclei with $I = 3/2$ located at nonzero local electric field gradient [19]. An additional stretching factor β is needed for temperatures below $T \sim 40$ K for the observable distribution of the relaxation. For $1/^{11}T_2$, the echo intensity decay can be well reproduced by the function, $M(2\tau) = M(0)\exp(-2\tau/T_2)$ (τ is the time interval between $\pi/2$ and π pulse), for the studied temperature range. This demonstrates that the transverse dephasing is mainly contributed by the spin fluctuations via the Redfield mechanism [20] instead of indirect and dipole coupling between nuclei, which will result in a Gaussian component [21]. For the high-temperature region of $T > 20$ K, the NMR relaxation rates $1/^{11}T_1$ and $1/^{11}T_2$ share a very similar temperature dependence; they first increase slightly, then tend to level off, and, finally, bend over with the sample cooling down. A wide hump peaked at $T \sim 30$ K is observed in both relaxation rates.

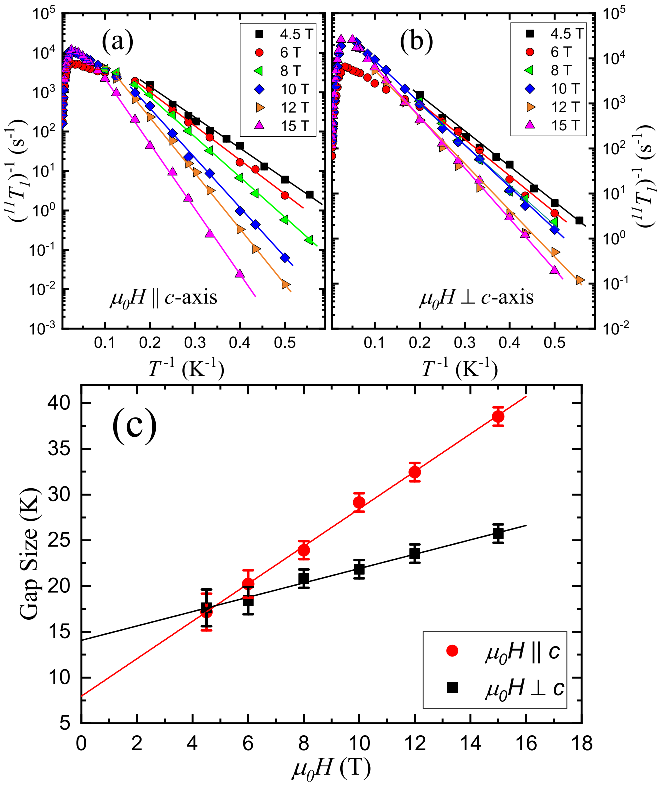

FIG. 4. Arrhenius plot of $1/^{11}T_1$ versus inverse temperature $1/T$ for magnetic fields along (a) or perpendicular to (b) the c axis. Solid lines are linear fits to the data. (c) Field dependence of the spin excitation gap in kelvins. Solid lines are fits to $\Delta(H) = \Delta_0 + g\mu_B H$.

The high-temperature hump is contributed by the crystal electric field (CEF)-related excitations. The magnetic behavior of rare-earth ions strongly depends on the local CEF which they occupy. The $(2J+1)$-fold degenerate states of $4f$ electrons are lifted by a certain CEF. For the non-Kramers ion $Pr^{3+}$with $J = 4$, the crystal field interactions lead to nine singlet states with possible accidental or near-degeneracies [22]. The mildly increasing $1/^{11}T_1$ and $1/^{11}T_2$ at high temperatures directly connect with the slowing-down of spin fluctuations of electrons occupying thermally activated CEF levels [15,23]. The wide hump results from the reduced thermal population at low temperatures, consistent with the slope change observed in dc susceptibility [11].

More intriguing is the low-temperature spin dynamics dominated by the CEF ground state of Pr^{3+}. With the sample further cooling from $T = 10$ K, $1/^{11}T_1$ drops steeply with the temperature for all the applied fields [see Figs. 3(a) and 3(b)]. Actually, the temperature dependence of $1/^{11}T_1$ can be well described by the thermally activated equation $1/T_1 \propto \exp(-\Delta/T)$, with a finite spin gap Δ. The gapped spin excitations under magnetic fields are better demonstrated by the Arrhenius plot, i.e., $1/^{11}T_1$ versus inverse temperature on a semilogarithmic scale as shown in Figs. 4(a) and 4(b). The field dependence of the gap size is shown in Fig. 4(c) for both field orientations. In sharp contrast, the temperature dependence of $1/^{11}T_2$ at $T < 10$ K completely deviates from that of $1/^{11}T_1$. A prominent peak around $T^* \sim 4$ K is observed, which is unusual in strongly correlated electron systems. When the magnetic field strength increases, the peak is suppressed and shifts to a little higher temperature, which is more pronounced for fields along the c axis.

IV. DISCUSSIONS AND CONCLUSIONS

We discuss the spin excitation property in Pr_3BWO_9 implied by our data. The low-temperature Knight shifts show a Curie-Weiss upturn behavior, while a contrasting gapped behavior is observed in $1/^{11}T_1$ with the sample cooling down. By roughly extrapolating the field dependence of the gap size [see Fig. 4(c)], a nonzero spin gap should also exist at zero field. In other words, this excitation gap is not field induced but inherent. The Knight shift, expressed as $K \propto A_{\mathrm{hf}}\chi(\mathbf{q}=0)$, measures the spin excitation at the wave vector $\mathbf{q} = 0$ [12,13]. The hyperfine coupling constant A_{hf} is negative in the present sample. However, the $1/^{11}T_1$ is contributed by the dynamic spin susceptibility summed over the whole reciprocal $\mathbf{q}$ space, which can be formulated as $1/T_1 \propto T\sum_{\mathbf{q}} |A(\mathbf{q})|^2[\chi''(\mathbf{q}, \omega_L)]/\omega_L$ [12,13]. The ω_L denotes the Larmor frequency, which can be treated as 0 in condensed matter physics. Thus, the contrasting low-temperature behavior of $1/^{11}T_1$ indicates strongly $\mathbf{q}$-dependent spin excitation, and the gap opens at a nonzero wave vector. In such an antiferromagnet with moderate coupling strength, this result actually suggests spin excitation gaps at the antiferromagnetic wave vector.

The obvious $\mathbf{q}$-dependent spin excitation in Pr_3BWO_9 is very different from that in the most investigated spin liquid candidate, $ZnCu_3(OH)_6Cl_2$. A fractional excitation continuum is observed by inelastic neutron scattering in the latter compound [3]. In recent NMR results [24], the spin-gapped behavior is observed in both Knight shifts and spin-lattice relaxations, which further indicates a gapped spin liquid state in $ZnCu_3(OH)_6Cl_2$. Additionally, the spin gap is suppressed by the applied magnetic field due to the Zeeman effect, whose slope corresponds to spinons with $S = 1/2$. Similar results are observed in its counterpart $Cu_3Zn(OH)_6FBr$ [25]. Supposing that spin liquid states do exist in these materials, the spin gap originates from the majority of short-ranged valence bonds.

There exist short-ranged collective spin excitations in the present sample. In contrast to the gapped behavior observed at a low temperature, $1/^{11}T_1$, a sharp peak is observed in the nuclear spin-spin relaxation rate $(1/^{11}T_2)$ at $T^* \sim 4$ K. The spin fluctuation contribution to $(1/^{11}T_2)$ through the Redfield mechanism can be expressed as $1/T_2^{\mathrm{Redfield}} = 1/T_2' + 1/(2T_1)$ [12]. The first term describes the in-plane decoherence contributed by the fluctuations of the longitudinal hyperfine field. The latter one has the same origination as $1/^{11}T_1$, both from the transverse hyperfine field fluctuations. Thus, the different behavior at low temperatures apparently results from the fluctuating hyperfine field anisotropy.

Understanding how longitudinal fluctuations contribute $1/T_2'$ supplies the key ingredient for revealing the spin excitation property. In the two-pulse Hahn echo experiment, dephasing of the transverse nuclear magnetization during the timing interval between pulses is refocused by applying the second π pulse after an equal time interval. If there exists some kind of dynamically inhomogeneous longitudinal field with a typical frequency of kilohertz, the changed local magnetic field will give rise to the failure of refocusing and, also, a decreased echo intensity. One typical example of this effect is the well-known vortex in type II superconductors under a magnetic field [26]. Measurements of $1/T_2$ have supplied another novel approach to study of the vortex dynamics in both cuprates and iron-based high-T_C superconductors [27–29]. The vortex core movement contributes an enhanced relaxation very similar to that observed here. Another example is fluids in a pore space. The spin-spin relaxation is obviously faster than that in pure fluids, which is enhanced by the interactions between nuclei and pore walls or paramagnetic centers [30]. Thus, the enhanced $1/T_2$ should be related to excitations of typical collective characteristics.

In other distorted kagome systems, $Nd_3Ga_5SiO_{14}$ and $Pr_3Ga_5SiO_{14}$, electron spin resonance studies have revealed collective spin excitations instead of the long-range continuum [31,32]. In $Pr_3Ga_5SiO_{14}$, dynamical short-range ordering is suggested by diffuse neutron-scattering observations [23]. μSR experiments indicate a fluctuating collective paramagnetic ground state in $Nd_3Ga_5SiO_{14}$ [33]. From the NMR experiments, a wipeout of the ^{71}Ga NMR signal below $T = 25$ K is observed in $Nd_3Ga_5SiO_{14}$ [33], resulting from the enhanced $1/T_2$. In $Pr_3Ga_5SiO_{14}$, the enhanced $1/T_2$ at low temperatures is also observed by NMR [23], although the physical connection between them is not pointed out. In the present Pr_3BWO_9, our observations provide unambiguous local evidence for short-ranged collective excitations. We stress that the short-range correlation still is dynamic in the time scale of NMR for the studied magnetic field range, as no abrupt change is observed in the temperature dependence of NMR spectra. This is in sharp contrast with what occurs in $Nd_3Ga_5SiO_{14}$, where field-induced partial magnetic order is identified by neutron scattering and heat transport [34,35].

The field dependence of the spin excitation gap can be understood with a simple theoretical model. Based on the assumption that Pr^{3+} also possesses the $S = 1$ spin state as occurs in $Pr_3Ga_5SiO_{14}$ [36], the Hamiltonian of the spin system considering only the single-ion anisotropy and antiferromagnetic exchange coupling can be roughly written as [31]

$$H = D\sum_i (S_i^z)^2 + g\mu_B B\sum_i S_i^z + J\sum_{i,j}\left[S_i^z S_j^z + \frac{1}{2}(S_i^+ S_j^- + S_i^- S_j^+)\right].$$

D and $J > 0$, respectively, denote the single-ion anisotropy and antiferromagnetic exchange coupling strength. Ignoring the magnetic frustration effect is believed not to change the qualitative main predictions [31]. For short-ranged excitation, results can be reached for two cases based on the linearized spin-wave approximation. (i) For $D > nJ$ (n is the number of nearest neighbors), the excitation energy spectrum is given by $\Delta E(\overrightarrow{k}) = D \mp g\mu_B B + nJ\gamma_{\overrightarrow{k}}$, where $\gamma_{\overrightarrow{k}}$ is the structure factor. (ii) For $D < 0$, the excitation energy is $\Delta E(\overrightarrow{k}) = (nJ + |D|)\sqrt{1-(\lambda\gamma_{\overrightarrow{k}})^2} + g\mu_B B$. In both cases, the spin excitation gap Δ at zero field is given by $\Delta(0) \sim nJ + |D|$. As predicted by case (i), the spin excitation gap will first decrease to 0 and then increase linearly with the applied magnetic field, while the gap size will only increase linearly with the field intensity in the $D < 0$ case.

In Fig. 4(c), we show the field dependence of the spin excitation gap in the present Pr_3BWO_9 sample. The linear fittings to the monotonically increasing gap size yield $\Delta(0) = 8.0$ K and $g = 3.047$ for $\mu_0 H || c$ axis and $\Delta(0) = 14.1$ K and $g = 1.167$ for $\mu_0 H \perp c$ axis. The monotonic field dependence of the gap size, the positive intercept, and the much larger g factor along the crystalline c axis all support the $D < 0$ case, where the $S^z = \pm 1$ state is energetically favorable. The comparatively large $\Delta(0)$ with the Curie-Weiss temperature should result from the pronounced single-ion anisotropy.

The single-ion anisotropy (determined by D) can be further qualitatively understood by the spin-orbit coupling effects ($\hat{H}_{\mathrm{SOC}} = \lambda\hat{\mathbf{S}}\cdot\hat{\mathbf{L}}$) in perturbation theory [37,38]. The spin orientation preference is determined by the local energy state of PrO_8 polyhedra, i.e., the combination of spin states, highest occupied molecular orbital (HOMO) and lowest unoccupied molecular orbital (LUMO). For a HOMO and LUMO with the same spin state, the spins prefer the $||z$ direction when the change in the orbital magnetic quantum number $|\Delta L_z| = 0$ but prefer the $\perp z$ direction when $|\Delta L_z| = 1$. For a HOMO and LOMO with different spin states, the situation for $|\Delta L_z| = 0$ and $|\Delta L_z| = 1$ is reversed. Thus, it is essential to further identify the CEF splittings of PrO_8 polyhedra and perform stricter theoretical simulation as that in $GdInO_3$ [39].

The ground state of Pr_3BWO_9 is neither magnetic ordered nor quantum spin liquid state, at least for the present temperature range. Collective spin excitations based on spin clusters or loops exist in the sample, which is still dynamic for the studied temperature and field range. Strong **q**-dependent behavior of the spin excitations is unambiguously evidenced by the contrasting temperature dependence of Knight shifts and spin-lattice relaxation rates. These are distinctively different from the long-range continuum excitations in quantum spin liquids. Within these constraints, Pr_3BWO_9 may be regarded as a cooperative paramagnet [40].

In conclusion, we have performed a detailed NMR study on the newly synthesized distorted kagome spin system Pr_3BWO_9. A cooperative paramagnetic state persists down to $T = 0.09$ K, far below its Curie-Weiss temperature, yielding a strong frustration effect. The unconventional short-ranged collective spin excitation is identified by comparatively studying the temperature dependence of Knight shifts, spin-lattice relaxation rates, and spin-spin relaxation rates. A spin gap opened at the antiferromagnetic wave vector is suggested by our data, whose size further shows a linear field dependence. This short-ranged collective spin excitation with a distinct **q**-dependent spin gap is totally different from the short-ranged valence bonds proposed in the spin liquid state. Our experiments reveal a highly unconventional spin excitation mode in frustrated antiferromagnets. Moreover, we have supplied a new approach to detecting collective spin excitations in magnetic materials.

ACKNOWLEDGMENTS

This research was supported by the National Key Research and Development Program of China (Grant No.

2016YFA0401802), the National Natural Science Foundation of China (Grants No. 11874057, No. 11874158, No. U1732273, and No. 21927814), and the Users with Excellence Program of Hefei Science Center CAS (Grant No. 2019HSC-UE008). A portion of this work was supported by the High Magnetic Field Laboratory of Anhui Province.

[1] L. Balents, Nature (London) **464**, 199 (2010).
[2] M. R. Norman, Rev. Mod. Phys. **88**, 041002 (2016).
[3] T. H. Han, J. S. Helton, S. Chu, D. G. Nocera, J. A. Rodriguez-Rivera, C. Broholm, and Y. S. Lee, Nature (London) **492**, 406 (2012).
[4] T. Imai, M. Fu, T. H. Han, and Y. S. Lee, Phys. Rev. B **84**, 020411(R) (2011).
[5] Z. L. Dun, J. Trinh, K. Li, M. Lee, K. W. Chen, R. Baumbach, Y. F. Hu, Y. X. Wang, E. S. Choi, B. S. Shastry, A. P. Ramirez, and H. D. Zhou, Phys. Rev. Lett. **116**, 157201 (2016).
[6] J. A. M. Paddison, H. S. Ong, J. O. Hamp, P. Mukherjee, X. J. Bai, M. G. Tucker, N. P. Butch, C. Castelnovo, M. Mourigal, and S. E. Dutton, Nat. Commun. **7**, 13842 (2016).
[7] Z. Dun, X. Bai, J. A. M. Paddison, E. Hollingworth, N. P. Butch, C. D. Cruz, M. B. Stone, T. Hong, F. Demmel, M. Mourigal, and H. Zhou, Phys. Rev. X **10**, 031069 (2020).
[8] C. Wellm, J. Zeisner, A. Alfonsov, M.-I. Sturza, G. Bastien, S. Gaß, S. Wurmehl, A. U. B. Wolter, B. Büchner, and V. Kataev, Phys. Rev. B **102**, 214414 (2020).
[9] Z. F. Ding, Y. X. Yang, J. Zhang, C. Tan, Z. H. Zhu, G. Chen, and L. Shu, Phys. Rev. B **98**, 174404 (2018).
[10] Z. Ma, Z.-Y. Dong, S. Wu, Y. Zhu, S. Bao, Z. Cai, W. Wang, Y. Shangguan, J. Wang, K. Ran, D. Yu, G. Deng, R. A. Mole, H.-F. Li, S.-L. Yu, J.-X. Li, and J. Wen, Phys. Rev. B **102**, 224415 (2020).
[11] M. Ashtar, J. J. Guo, Z. T. Wan, Y. Q. Wang, G. S. Gong, Y. Liu, Y. L. Su, and Z. M. Tian, Inorg. Chem. **59**, 5368 (2020).
[12] C. P. Slichter, *Principles of Magnetic Resonance* (Springer, Berlin, 1990).
[13] A. Abragam, *The Principles of Nuclear Magnetism* (Oxford University Press, Oxford, UK, 1961).
[14] See Supplemental Material at http://link.aps.org/supplemental/10.1103/PhysRevB.104.155150 for the temperature dependence of single-crystal dc susceptibility and ultralow-temperature specific heat.
[15] K. Y. Zeng, L. Ma, Y. X. Gao, Z. M. Tian, L. S. Ling, and L. Pi, Phys. Rev. B **102**, 045149 (2020).
[16] M. Baenitz, P. Schlender, J. Sichelschmidt, Y. A. Onykiienko, Z. Zangeneh, K. M. Raniith, R. Sarkar, L. Hozoi, H. C. Walker, J.-C. Orain, H. Yasuoka, J. van den Brink, H. H. Klauss, D. S. Inosov, and T. Doert, Phys. Rev. B **98**, 220409(R) (2018).
[17] M. M. Bordelon, E. Kenney, C. Liu, T. Hogan, L. Posthuma, M. Kavand, Y. Lyu, M. Sherwin, N. P. Butch, C. Brown *et al.*, Nat. Phys. **15**, 1058 (2019).
[18] J. C. Zheng, K. J. Ran, T. R. Li, J. H. Wang, P. S. Wang, B. Liu, Z. X. Liu, B. Normand, J. S. Wen, and W. Yu, Phys. Rev. Lett. **119**, 227208 (2017).
[19] A. Narath, Phys. Rev. **162**, 320 (1967).
[20] A. G. Redfield, Phys. Rev. **98**, 1787 (1955).
[21] M. Takigawa, N. Motoyama, H. Eisaki, and S. Uchida, Phys. Rev. B **57**, 1124 (1998).
[22] A. Scheie, M. Sanders, J. Krizan, A. D. Christianson, V. O. Garlea, R. J. Cava, and C. Broholm, Phys. Rev. B **98**, 134401 (2018).
[23] L. L. Lumata, T. Besara, P. L. Kuhns, A. P. Reyes, H. D. Zhou, C. R. Wiebe, L. Balicas, Y. J. Jo, J. S. Brooks, Y. Takano, M. J. Case, Y. Qiu, J. R. D. Copley, J. S. Gardner, K. Y. Choi, N. Dalal, and M. J. R. Hoch, Phys. Rev. B **81**, 224416 (2010).
[24] M. X. Fu, T. Imai, T. H. Han, and Y. S. Lee, Science **350**, 655 (2015).
[25] Z. L. Feng, Z. Li, X. Meng *et al.*, Chin. Phys. Lett. **34**, 077502 (2017).
[26] B. J. Suh, D. R. Torgeson, and F. Borsa, Phys. Rev. Lett. **71**, 3011 (1993).
[27] C. H. Recchia, J. A. Martindale, C. H. Pennington, W. L. Hults, and J. L. Smith, Phys. Rev. Lett. **78**, 3543 (1997).
[28] L. Bossoni, P. Carretta, A. Thaler, and P. C. Canfield, Phys. Rev. B **85**, 104525 (2012).
[29] A. Rigamonti, F. Borsa, and P. Carretta, Rep. Prog. Phys. **61**, 1367 (1998).
[30] J. Korringa, D. O. Seevers, and H. C. Torrey, Phys. Rev. **127**, 1143 (1962).
[31] S. Ghosh, S. Datta, H. D. Zhou, M. J. R. Hoch, C. R. Wiebe, P. Schlottmann, and S. Hill, Phys. Rev. B **88**, 094414 (2013).
[32] S. Ghosh, S. Datta, H. D. Zhou, M. J. R. Hoch, C. R. Wiebe, P. Schlottmann, and S. Hill, Phys. Rev. B **90**, 224405 (2014).
[33] A. Zorko, F. Bert, P. Mendels, P. Bordet, P. Lejay, and J. Robert, Phys. Rev. Lett. **100**, 147201 (2008).
[34] H. D. Zhou, B. W. Vogt, J. A. Janik, Y.-J. Jo, L. Balicas, Y. Qiu, J. R. D. Copley, J. S. Gardner, and C. R. Wiebe, Phys. Rev. Lett. **99**, 236401 (2007).
[35] Q. J. Li, Z. Y. Zhao, H. D. Zhou, W. P. Ke, X. M. Wang, C. Fan, X. G. Liu, L. M. Chen, X. Zhao, and X. F. Sun, Phys. Rev. B **85**, 174438 (2012).
[36] P. Bordet, I. Gelard, K. Marty, A. Ibanez, J. Robert, V. Simonet, B. Canals, R. Ballou, and P. Lejay, J. Phys.: Condens. Matter **18**, 5147 (2006).
[37] H. Xiang, C. Lee, H.-J. Koo, X. Gong, and M.-H. Whangbo, Dalton Trans. **42**, 823 (2013).
[38] M.-H. Whangbo, E. E. Gordon, H. Xiang, H.-J. Koo, and C. Lee, Acc. Chem. Res. **48**, 3080 (2015).
[39] X. Q. Yin, Y. L. Li, G. H. Wang *et al.*, in press (2021).
[40] J. Villain, Z. Phys. B **33**, 31 (1979).